IOPscience iopscience.iop.org

Home Search Collections Journals About Contact us My IOPscience

On inversion of normal metal tunnelling data

This article has been downloaded from IOPscience. Please scroll down to see the full text article.

1994 J. Phys.: Condens. Matter 6 6637

(http://iopscience.iop.org/0953-8984/6/33/011)

View the table of contents for this issue, or go to the journal homepage for more

Download details:
IP Address: 171.66.16.151
The article was downloaded on 12/05/2010 at 20:19

Please note that terms and conditions apply.

J. Phys.: Condens. Matter 6 (1994) 6637–6650. Printed in the UK

On inversion of normal metal tunnelling data

J J Wnuk

Institute of Low Temperature and Structure Research, Polish Academy of Sciences, Okolna 2, 50-422 Wroclaw, Poland

Received 10 December 1993, in final form 21 March 1994

Abstract. A short summary of the theoretical and experimental status of elastic tunnelling between normal metals is given. Methods for the determination of the electron–phonon interaction function, $\alpha^2F(\omega)$, from the conductance, $\sigma(\omega)$, of a normal metal tunnel junction are presented and their performance is discussed. A complete list of sum rules applicable to the inversion procedures is given for the first time. Elimination of the thermal smearing of the conductance data with the help of the fast Fourier transform algorithm and the regularization method is described. The possibility of the existence of 'interference' between the elastic and inelastic parts of the tunnelling current is discussed for conductivity data of Pb and Sn.

1. Introduction

Starting from the paper of Svistunov *et al* [1], fresh attention has been paid to the problem of tunnelling between the electrodes of normal metals, as it became possible to derive the frequency dependence of the electron–phonon coupling function from tunnelling conductivity data. The dependence of the odd part of the conductivity, $\sigma_-(\omega) = [\sigma(\omega) - \sigma(-\omega)]/2$, on the real part of the phonon-induced electron self-energy, $\Sigma(\omega) = \Sigma_1(\omega) + i\Sigma_2(\omega)$, was postulated by Hermann and Shmid in 1968 to have the form [2]:

$$\sigma_-(eV) = -(\alpha_{HS}\sigma_0/\mu)[\Sigma_1^a(eV) - \Sigma_1^b(-eV)]. \tag{1}$$

The superscripts a and b denote the two normal electrodes of a tunnel junction, α_{HS} was estimated in [2] to be of order 30, μ is the chemical potential, V is the applied voltage ($eV = \omega, \hbar = 1$) and σ_0 is the tunnelling conductance in the absence of self-energy effects. Equation (1) has been obtained assuming a weak energy dependence of the tunnelling matrix element.

The presence of the self-energy-induced structure in the tunnelling conductivity has been corroborated experimentally by Rowell *et al* [3] and Burrafato *et al* [4], and more recently by Svistunov *et al* [1] and Chernyak *et al* [5]. The experimental value of the constant α_{HS} is of order unity [1, 3], much less than estimated in [2]; but applying the two-band model of the barrier insulator, α_{HS} is replaced by $\alpha \ll \alpha_{HS}$ [1]. Still, there arises a question whether an electron tunnels at its bare band-structure energy, as was assumed in [2], or the energy should be renormalized to include the many-body effects in the tunnelling matrix element. Appelbaum and Brinkman [6], working from the latter, have shown that no self-energy effects remain in the odd part of the conductivity when renormalization takes place. For a simple model, Davis [7] came to the same conclusion without using the transfer Hamiltonian approach. As renormalization of the electron energy seems to be necessary

0953-8984/94/336637+14$19.50 © 1994 IOP Publishing Ltd

[6, 7], the effects observed in [1, 3–5] should be due to something other than the exponential part of the tunnelling matrix element. Appelbaum and Brinkmann [6] suggested that the structure observable in the odd part of the tunnelling conductance is caused by a weak momentum dependence of the self-energy or the pre-exponential factors of the tunnelling matrix element. Leavens [8], assuming the weak momentum dependence of the electron self-energy, has derived a formula very similar to (1):

$$\sigma_-(eV) = -\sigma_0[(\gamma_a/\mu_a)\Sigma_1^a(eV) - (\gamma_b/\mu_b)\Sigma_1^b(-eV) - \delta eV]. \tag{2}$$

Here $\gamma_{a,b}$ is a constant of order unity, and δ depends on the properties of both electrodes. The barrier-dependent parameter α does not appear in (2) since it has been assumed that α is the same for both sides of the barrier. However, the barrier asymmetry should be reflected in (2) at least when the phonon spectra of the two metal electrodes show up in the same energy range [3].

One may question the role of the 'interference' term, which, according to [9], should appear in the tunnelling conductance together with the elastic and inelastic contributions. Belogolovskii *et al* [10, 11] explain the frequency-dependent dumping of the odd conductance curve of an Al–I–Sn junction [4] by the existence of this additional term. The 'interference' contribution has the same symmetry and is of the same order as the elastic one, but has opposite sign. The net effect on the odd part of the tunnelling conductance is that it, like the electron–phonon coupling, would be weakened at higher frequencies:

$$\alpha^2F(\omega) \to [1 - \phi(\omega)]\alpha^2F(\omega). \tag{3}$$

Here, $\phi(\omega)$ is a smooth function, normalized to unity, that increases with frequency. One may interpret this effect as a partial 'undressing' of the tunnelling electrons from the many-body interactions characteristic of the bulk electrode [12].

There is a set of superconducting materials expected to have a sharp structure in the electronic density of states near the Fermi energy. Among them are the A15 compounds and Chevrel phases. Such a structure should have an apparent effect on the conductance of the normal metal tunnelling junctions [13]. In this case the symmetry of the electron self-energy is deviated and the odd part of the conductance of the normal metal tunnelling junction additionally contains information about the electronic density of states, $\tilde{N}(\omega)$ [13, 14].

A serious problem in measurements of the normal metal tunnelling junction characteristics is thermal smearing of halfwidth $5.4k_BT$ (k_B is the Boltzmann constant), which, for example, completely smears the structure of the electron–phonon coupling function of Sn at $T = 4.2$ K (figure 1). Leavens, motivated by work of Hertel and Orlando [16], has recently derived an inversion formula allowing elimination of thermal smearing [17]. Unfortunately, this formula is very sensitive to errors in the conductance data [17, 18].

The problems and questions listed above will be discussed in the subsequent sections of this work.

2. Tunnelling conductivity

In view of the previous comments, several effects should be reflected in the formula for the conductivity of the normal metal tunnelling junction. However, even the general shape of the conductivity of the planar junctions is described by the theoretical models with an

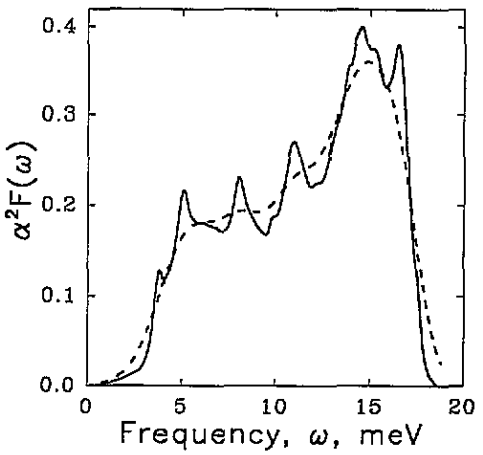

Figure 1. The Eliashberg function, $\alpha^2F(\omega)$, of Sn (after [15]) (full curve) and the illustration of thermal smearing of $\alpha^2F(\omega)$ at $T = 4.2$ K (broken curve).

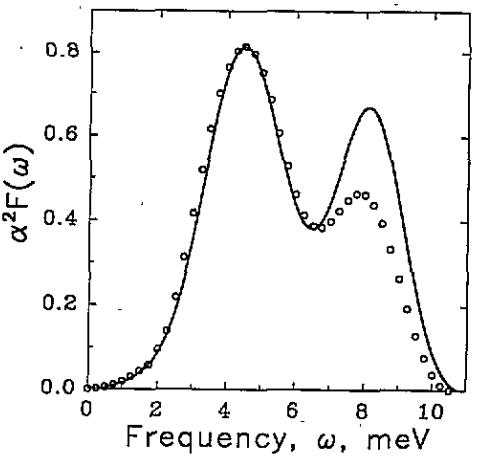

Figure 2. The electron–phonon interaction function, $\alpha^2F(\omega)$, of Pb calculated from the data of [3] (open circles) and simulated for the same 'experimental' conditions (full curve).

accuracy of a few per cent only. This is caused by the complicated shape of the tunnel barrier in the real junctions. Assumption of a trapezoidal barrier gives similar results within different models [20]. Both the diffuse and sharp metal–insulator interface approximations lead to a conductivity that is parabolic with voltage. The general picture is not affected by inclusion of effects due to image forces (lowering of the barrier and smearing of its edges). An important feature is the shift of the minimum of $\sigma(eV)$ from zero voltage owing to barrier asymmetry. Unfortunately, the experimentally observed shifts are sometimes larger than predicted by the model for any reasonable barrier parameters. This can be explained by the presence of organic impurities in the oxides forming the tunnelling barrier [20, 21].

The shape of the normal metal tunnel junction conductivity is described with 10% accuracy, in the voltage region $|V| < 0.4$ V, by a simple formula:

$$\sigma(eV) = \sigma(0) + aeV + b(eV)^2 \tag{4}$$

where a and b are constants depending on the barrier parameters. This, however, is valid only for small shifts of the conductivity minimum. An interesting observation is that, at least in some cases, this approximation describes the conductivity data better than the exact models [20], i.e. the experimental tunnelling conductivity is more parabolic than the exact solutions would suggest.

To the overall shape of the tunnelling conductivity should be added contributions coming from excitation of vibrational modes due to impurities in the oxide layer [22], the oxide itself [23] and the metal electrodes [3]. The inelastic tunnelling processes are well known and are successfully used, for example, for investigations of the vibrational spectra of molecules [24]. Fortunately, these contributions are symmetric against zero voltage and should not be reflected in the odd part of the tunnelling conductivity.

One may choose the two different metal electrodes of the tunnel junction in such a way that $\alpha^2F_a(\omega) \gg \alpha^2F_b(\omega)$ in the frequency range characteristic to $\alpha^2F_a(\omega)$. Assuming further that γ_a/μ_a is comparable to or greater than γ_b/μ_b, the self-energy effects of metal b in the odd part of the tunnelling conductivity described by equation (2) may be neglected.

This would lead to a simple proportionality between $\sigma_-(eV)$ and $\Sigma_1^a(eV)$ if not for the linear terms deduced from (2) and (3). Let us define the experimental conductivity, $\sigma_-^e(eV)$, as

$$\sigma_-^e(eV) \equiv \sigma_-(eV) + aeV \tag{5}$$

where

$$\sigma_-(eV) = -\sigma_0(\gamma/\mu)\Sigma_1(eV) \tag{6}$$

and the constant a now contains all the contributions linear with voltage. (Notice that some of the indices are skipped as they are no longer necessary.) Thus, having measured the conductivity of the normal metal tunnel junction consisting of appropriately chosen metals, one can derive the real part of the electron self-energy in one of the electrodes, providing one finds a way to eliminate the linear part of $\sigma_-^e(eV)$. The inversion methods presented below serve to extract further information (frequency dependence of $\alpha^2F(\omega)$) from the tunnelling data.

3. Inversion methods

Coming from the well known result for the phonon contribution to the electron self-energy,

$$\Sigma(\omega) = \int_0^{\omega_0} d\nu\, \alpha^2F(\nu) \ln\left|\frac{\nu-\omega}{\nu+\omega}\right| - i\pi \int_0^{|\omega|} d\nu\, \alpha^2F(\nu) \tag{7}$$

obtained from the Eliashberg equations at zero temperature [19], Svistunov *et al* [1] derived a formula that may be updated to the form

$$\alpha^2F(\omega) = \frac{2\mu\omega}{\gamma\sigma_0\pi^2} \int_0^{\infty} \frac{d\sigma_-(\nu)}{d\nu} \frac{d\nu}{\omega^2-\nu^2}. \tag{8}$$

We have recently proposed a similar formula connecting the Eliashberg function directly with the odd part of the tunnelling conductivity [18]

$$\alpha^2F(\omega) = -\frac{\mu}{\sigma_0\gamma}\frac{4\omega}{\pi^2} \int_0^{\infty} \frac{\nu\sigma_-(\nu)}{(\omega^2-\nu^2)^2}\, d\nu. \tag{9}$$

(For the derivation of (8) and (9) see appendix 1.)

As the upper limits of the integrals in (8) and (9) are infinite, an extrapolation of the conductivity data out of the experimental range is necessary. From (7) one can estimate that for $\omega \gg \omega_0$ (ω_0 denotes the phonon spectrum boundary):

$$\Sigma_1(\omega) \simeq -2\bar{E}/\omega - \lambda\langle\omega^4\rangle/3\omega^3 \tag{10}$$

$$d\Sigma_1(\omega)/d\omega \simeq 2\bar{E}/\omega^2 + \lambda\langle\omega^4\rangle/\omega^4. \tag{11}$$

With sufficient accuracy, the last terms of the above equations may be omitted for $\omega_c \geqslant 3\omega_0$, and the constant $\bar{E}$ (for the definition of the constants see appendix 1) may be obtained from the continuity condition of $\sigma_-(\omega)$ (or its derivative) at ω_c. The only problem is that before doing so one has to remove the linear background from $\sigma_-^e(\omega)$, i.e. determine the constant a of relation (5). This can be done with the help of the sum rules derived from appropriate

dispersion relations (appendix 2). For clarity, the sum rules are listed in table 1. The first two of them are exact sum rules—for practical purposes more useful are the approximate ones with limited region of integration. Two of them, numbers 3 and 5 of table 1, are used to determine the constant a from, respectively, $\sigma_-^e(\omega)$ or $d\sigma_-^e(\omega)/d\omega = d\sigma_-(\omega)/d\omega + a$:

$$a = \frac{3}{2\omega_c}\left(\sigma_-^e(\omega_c) - \frac{1}{\omega_c^2}\int_0^{\omega_c} \omega\sigma_-^e(\omega)\,d\omega\right) \tag{12}$$

$$a = \frac{1}{2}\left(\frac{d\sigma_-^e(\omega)}{d\omega}\bigg|_{\omega=\omega_c} - \frac{1}{\omega_c}\int_0^{\omega_c}\frac{d\sigma_-^e(\omega)}{d\omega}\,d\omega\right). \tag{13}$$

The remaining sum rule, number 4 in table 1, gives the value of $\underline{A}^2 = A^2\gamma\sigma_0/\mu$,

$$\underline{A}^2 = \frac{2}{\pi^2}\left(\int_0^{\omega_c}\frac{\sigma_-^e(\omega)}{\omega}\,d\omega + \sigma_-^e(\omega_c)\right) \tag{14}$$

without need of calculating $\alpha^2F(\omega)$ from (8) or (9). (In fact, both inversion methods give only the function $G(\omega) = \alpha^2F(\omega)\gamma\sigma_0/\mu$.) Equation (14) allows one to determine the constant γ whenever the value of A^2 is known (from superconductive tunnelling, for example).

Table 1. Sum rules for the electron self-energy and its derivative.

No	Sum rule
1	$\int_0^\infty \mathrm{Re}\frac{d\Sigma(\omega)}{d\omega}\,d\omega = 0$
2	$\int_0^\infty \Sigma_I(\omega)\frac{d\omega}{\omega} = -\frac{\pi^2A^2}{2}$
3	$\int_0^{\omega_c} \omega\Sigma_I(\omega)\,d\omega \simeq -2\bar{E}\omega_c - \frac{\lambda\langle\omega^4\rangle}{3\omega_c}$
4	$\int_0^{\omega_c} \Sigma_I(\omega)\frac{d\omega}{\omega} \simeq 2\frac{\bar{E}}{\omega_c} - \frac{\pi^2A^2}{2} + \frac{\lambda\langle\omega^4\rangle}{9\omega_c^3}$
5	$\int_0^{\omega_c} \mathrm{Re}\frac{d\Sigma(\omega)}{d\omega}\,d\omega \simeq -2\frac{\bar{E}}{\omega_c} - \frac{\lambda\langle\omega^4\rangle}{3\omega_c^3}$

The following property is useful for scaling of the initial data

$$\lim_{\omega\to 0}\frac{\Sigma_I(\omega)}{\omega} = \frac{d\Sigma_I(\omega)}{d\omega}\bigg|_{\omega=0} = -\lambda. \tag{15}$$

Thus, having measured the conductivity $\sigma(\omega)$, or its derivative $d\sigma(\omega)/d\omega$, of a tunnel junction in the region $(-\omega_c, \omega_c)$, $\omega_c \geqslant 3\omega_0$, one may calculate the frequency dependence of the electron–phonon interaction function, $\alpha^2F(\omega)$.

It should be stressed that, although the two versions of the inversion method for normal metal tunnelling data are mathematically equivalent, formula (8) should be used only when $d\sigma_-(\omega)/d\omega$ is directly available, as the numerical differentiation of noisy $\sigma_-(\omega)$ data is always somewhat arbitrary. Still, the character of the convergence of the integrals in (9) and (8) is the same. This means that the cut-off energy, ω_c, at which one may start the extrapolation of $\sigma_-(\omega)$ and, respectively, $d\sigma_-(\omega)/d\omega$, is the same in both cases. Calculations performed for both versions of the method have shown that ω_c may be as low as $2\omega_0$ without

noticeable loss of accuracy. However, to get, accurately enough, the constant a from (12) or (13), the respective experimental data up to energy $\omega_c \geqslant 3\omega_0$ are needed (this is a consequence of taking into account only the first terms of the approximations (10) and (11) while deriving relations (12) and (13)). Because of the different denominators in the integrands of (9) and (8), the integrand of formula (9) has to be calculated more accurately, but in a narrower frequency region around ω, which in effect speeds up the numerical calculations.

4. Thermal smearing

The derivatives of the tunnelling current are measured using the well known modulation technique—by harmonic detection of the current induced by a small AC voltage supplied to the tunnel junction together with the constant biasing voltage V. Generally, the higher the harmonic, the smaller is the detected signal. The modulation voltage, V_ω, should be as small as possible to minimize the smearing of the experimental curve that it causes (its halfwidth equals $1.73\ eV_\omega$ or $1.22\ eV_\omega$ in the case of, respectively, $\sigma(\omega)$ and $d\sigma(\omega)/d\omega$ measurements). This smearing adds geometrically to the significant thermal broadening of the halfwidth of $5.4k_BT$ characteristic for both $\sigma(\omega)$ and $d\sigma(\omega)/d\omega$. Another source of broadening of the Eliashberg function is experimental error, unavoidable in such subtle experiments, and consecutive averaging (smoothing) of the conductance, $\sigma_-(\omega)$ (or $d\sigma_-(\omega)/d\omega$), data. The magnitude of the experimental error may be decreased by increasing the modulation voltage, but, in effect, one may only balance between the two smearing components.

Leavens [17] has recently proposed an inversion formula for $\alpha^2F(\omega)$, which, based on the convolution theorem for the Fourier transform, eliminates the effect of thermal smearing of $d\sigma(\omega)/d\omega$. However, the existence of a substantial experimental error in normal metal tunnelling conductivity data drastically limits the usefulness of this formula. Furthermore, it seems to be more sensible to use very efficient FFT (fast Fourier transform) algorithms while solving the deconvolution problems, than to build an algorithm based on an analytical expression of [17] involving double integration. Moreover, there exist a class of mathematical methods, called regularization methods, allowing one to handle data perturbed by noise [26], and these methods are easy to use along with the discrete Fourier transform.

The elimination of the smearing of the tunnelling conductivity caused by the finite temperature comes to a stabilization of the 'ill-conditioned' problem of deconvolution. All the quantities met here; viz. $\Sigma(\omega)$, $\sigma(\omega)$ and $\alpha^2F(\omega)$, depend on temperature. The temperature dependence of $\alpha^2F(\omega)$ due to thermal expansion of the crystal lattice may be neglected at low temperatures, but the electron self-energy function [17]

$$\Sigma_1(\omega, T) = -\int_{-\infty}^{\infty} d\nu \int_0^{\infty} d\Omega\, \alpha^2F(\Omega) \left(\frac{f(-\nu)}{\nu - \omega + \Omega} + \frac{f(\nu)}{\nu - \omega - \Omega} \right) \tag{16}$$

and the odd part of the tunnelling conductivity

$$\sigma_-(\omega, T) = \sigma_0 \int_{-\infty}^{\infty} d\nu\, \frac{\gamma}{\mu} \Sigma_1(\nu, T) \frac{d f(\nu - \omega)}{d(\nu - \omega)} \tag{17}$$

depend much more strongly on temperature ($f(\omega)$ is the Fermi–Dirac distribution function). Thus, both the odd part of the conductivity and its derivative can be expressed at finite

temperature as a double convolution of their zero-temperature form, $\sigma_-(\omega) \equiv \sigma_-(\omega, T=0)$, $\mathrm{d}\sigma_-(\omega)/\mathrm{d}\omega \equiv \mathrm{d}\sigma_-(\omega, T=0)/\mathrm{d}\omega$, with the derivative of the distribution function,

$$\sigma_-(\omega, T) = \sigma_-(\omega) * \left(\frac{\mathrm{d}f(\omega, T)}{\mathrm{d}\omega}\right)^2. \tag{18}$$

Here, $g(\omega)*h(\omega) = \int \mathrm{d}\nu\, g(\nu)h(\nu-\omega)$, and the second power marks the double convolution.

Generally, one has to calculate the Fourier transform of the odd part of the conductivity, $\sigma_-(\omega, T)$ (or its derivative), and then divide it by

$$H(t, T) \equiv \mathcal{F}\left(\left(\frac{\mathrm{d}f(\omega, T)}{\mathrm{d}\omega}\right)^2\right) = \frac{2x^2}{\cosh(2x)-1} \qquad x = \pi k_B T t \tag{19}$$

where t is a 'time' variable. Without going into the details of the regularization method used, it is enough to state that it is a kind of optimization procedure with only one parameter, depending crucially on the estimate of the experimental error (see appendix 3). Fortunately, the Fourier transform gives a means of evaluation of the experimental error (this is not the error of the measurement of $\sigma^e(\omega, T)$ but the error characterizing $\sigma_-(\omega, T)$) as a weighted sum of the transform coefficients. As a result one obtains the most 'smooth' function from the class of solutions of the deconvolution task.

Thus, the full inversion procedure aimed at obtaining the frequency dependence of $\alpha^2F(\omega)$ from $\sigma(\omega, T)$ consists of the following steps:

(i) $\sigma_-^e(\omega, T)$ is obtained from measured $\sigma(\omega, T)$.

(ii) Constant a is calculated from (12) and $\sigma_-(\omega, T)$ is determined.

(iii) Constant $\bar{E}\gamma\sigma_0/\mu$ is estimated from the condition of continuity of $\sigma_-(\omega, T)$ at the cut-off frequency ω_c (also $\underline{A}^2$ and $\underline{\lambda} = \lambda\gamma\sigma_0/\mu$ may be estimated from (14) and (15)).

(iv) The regularized elimination of the thermal smearing is performed (in a degree determined by the experimental error) giving $\sigma_-(\omega)$.

(v) Function $G(\omega) = \alpha^2F(\omega)\gamma\sigma_0/\mu$ is calculated from (9).

We have implemented the above algorithm in a computer code and as testing data we used $\sigma(\omega, T)$ calculated from the values of $\alpha^2F(\omega)$ given for Pb and Sn in [30]. The thermal smearing was introduced according to equations (16) and (17), and the 'experimental' error was simulated by a random-number generator. The whole calculation loop $\alpha^2F(\omega) \to \sigma(\omega, T) \to \alpha^2F(\omega)$ closed with a very good agreement (within tenths of a per cent) when the 'experimental' error was kept zero.

5. Discussion

Both of the presented inversion methods represented by relations (8) and (9) may be successfully used to determine the frequency dependence of the electron–phonon interaction function when either the tunnelling conductivity, $\sigma(\omega, T)$, or its derivative are known in the range $(-3\omega_0, 3\omega_0)$. The elimination of thermal smearing may be applied both to $\sigma_-(\omega, T)$ and to $\mathrm{d}\sigma_-(\omega, T)/\mathrm{d}\omega$ to the same effect depending on the magnitude of the experimental error.

The experiments performed so far [1, 3–5] have shown that the electron self-energy effects are visible in the odd part of the tunnelling conductivity in the normal metal tunnelling junctions—at least for metals with strong electron–phonon interaction. However, the results

obtained for Pb and Sn, for which $\alpha^2(\omega)$ is known also from superconductive tunnelling spectroscopy, indicate the presence of some other phenomena not found in the previous experiments.

Already some time ago, Ivanchenko and Medvedev [9] together with Belogolovskii [10, 11] suggested that the tunnelling current flowing between two normal electrodes should consist of at least three terms (if we consider only the interactions between the tunnelling electrons and phonons),

$$I(eV) = I_{el}(eV) + I_i(eV) + I_{ie}(eV).$$

Two of them are known and come from *elastic* (I_{el}) and *inelastic* (I_{ie}) tunnelling channels. The *interference* term (I_i) effectively reduces the higher-frequency amplitude of the elastic contribution by having the same symmetry but opposite sign. One could interpret the *elastic* and *interference* terms together as the partial 'undressing' of the tunnelling electron from the many-body interaction [12], which is quite convincing knowing that in the case of normal metal junctions tunnelling electrons probe only a few atomic layers of the electrodes. However, it is not clear why the same should not be true for the inelastic tunnelling process. In fact, an attempt has been made to invert the inelastic tunnelling conductance of a normal metal junction to get the Eliashberg function [27, 28]. An experiment with an Al–I–Pb junction has shown that the *low*-frequency part of $\alpha^2F(\omega)$ is dumped (transverse peak of $\alpha^2F(\omega)$ spectrum of Pb). This was again explained as due to the metal–insulator interface and short depth to which tunnelling electrons probe the normal metal [27]. This line of reasoning could lead to a hypothesis that at the surface of a normal metal the probability weights of taking part in inelastic and elastic tunnelling processes are different for transverse and longitudinal phonons. It is probably accidental, but the ratios between the magnitude of the transverse to longitudinal peaks in $\alpha^2F(\omega)$ deduced from inelastic tunnelling experiment [27] and elastic one [3] (see figure 2) are exactly reversed. However, there may be still another explanation for the rounding and change of the relative magnitude of the electron–phonon interaction function of Pb obtained from the normal metal tunnelling—simply disorder present at the metal–insulator interface (compare figure 2 and the data of Knorr and Barth for amorphous Pb films [29]).

Thus, we are not convinced that the concept of the *interference* contribution to the tunnelling current explains the experimental data. Certainly, the shift of the maximum of $\sigma_-(\omega)$ to lower energies observed for Al–I–Sn junctions [4] can be explained by high-energy dumping of $\alpha^2F(\omega)$. Also the results of Rowell *et al* [3] suggest the same but to much smaller extent. The lowering of the second maximum of $\sigma_-(\omega)$ for Pb–I–Pb junctions cannot be explained by any type of smearing discussed in this paper. In fact, we used the data of [3] (read from figure 17 of that reference) to calculate the function $\alpha^2F(\omega)$. The result is shown in figure 2 together with a simulated one. To obtain the former we used $\alpha^2F(\omega)$ determined from superconductive tunnelling experiments [30] and computed $\Sigma_1(\omega)$ assuming the same magnitude of experimental error (for the same number of points) and the same amount of smearing caused by temperature and modulation voltage. Then the inversion method has been applied—similarly as for the original data. The agreement of both $\alpha^2F(\omega)$ curves up to about 6 meV is astonishing taking into account the low accuracy of the initial data. The second peak of the 'experimental' $\alpha^2F(\omega)$ is lowered in magnitude as the shape of $\sigma_-(\omega)$ suggested. Unfortunately, we could not perform the same calculations for the data of Svistunov *et al* [1] or Chernyak *et al* [5] as they presented their $\sigma_-(\omega)$ results only up to about ω_0. Still, the shape of $\alpha^2F(\omega)$ curve obtained for Pb in [1] may be well explained by the smearing caused by the temperature of 2.3 K and the modulation

amplitude of 0.3–1 mV (see figure 3), even when the experimental error is neglected. In case of $Pb_{70}Bi_{30}$ alloy, the structure of the obtained electron–phonon interaction function is even stronger than that resulting from superconductive tunnelling experiments [1]. An exception is $\alpha^2F(\omega)$ derived from the conductance of an Al–I–Bi junction where the low-frequency peak is much more pronounced that the rest of the spectrum. However, in this case, the estimated constant γ exceeds those obtained for other junctions by an order of magnitude. As long as this effect is not investigated, one cannot rule out the possibility of an explanation other than the interference contribution.

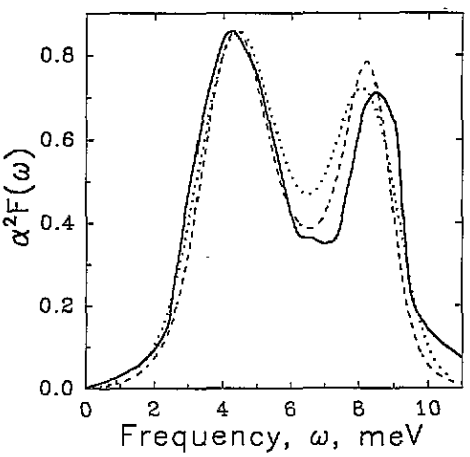

Figure 3. The electron-phonon interaction function, $\alpha^2F(\omega)$, of Pb (from [1]) (full curve), and calculated from superconductive tunnelling data [30] for $T = 2.3$ K and modulation amplitude of 0.3 mV (broken curve) and 1 mV (dotted curve).

The last problem we would like to discuss is the influence of the structure in the electronic density of states, $\tilde{N}(\omega)$, in the immediate vicinity of the Fermi level on the tunnelling conductance [13, 14]. Such sharp structure in $\tilde{N}(\omega)$ should cause symmetry deviation of the electron self-energy, and an inversion procedure of the kind presented here would not give a function proportional to $\alpha^2F(\omega)$ but a more complicated one:

$$G(\omega) = \frac{\mathrm{d}}{\mathrm{d}\omega}\int_0^{\omega} \mathrm{d}\Omega\,\alpha^2F(\omega-\Omega)\tfrac{1}{2}[\tilde{N}(\Omega)+\tilde{N}(-\Omega)] \qquad \omega > 0. \tag{20}$$

The apparent difference between $\alpha^2F(\omega)$ and $G(\omega)$ is a negative tail of the latter close to ω_0 and a relative shift of weight to lower frequencies [13, 14]. Unfortunately, no structure that could be attributed to the self-energy effects has been seen in the odd part of the conductivity of tunnel junctions with the A15 compounds in the normal state [31]. Even if one succeeded in such a measurement, it seems very probable that the effects of the sharp structure of $\tilde{N}(\omega)$ would be still unobservable in the distorted region near the metal–insulator interface to which the tunnelling effect, especially in normal metal junctions, is limited [14].

6. Conclusions

The inversion methods [1, 18] allow the extraction of the frequency dependence of the electron–phonon interaction function, $\alpha^2F(\omega)$, from the normal metal conductivity data taking into account only the elastic tunnelling channel. The account of other effects may be estimated by comparison of the functions $\alpha^2F(\omega)$ obtained from superconductive and normal metal tunnelling experiments performed on the same tunnel junction. Then, also the even part of $\sigma(eV)$ (measured in the normal state) could be used to derive $\alpha^2F(\omega)$ applying the method of [27]. In this way complementary data could be collected, finally resolving the problem of different tunnelling channels in a normal metal junction. What is still controversial is how accurately equation (4) describes a real tunnelling barrier. Brinkmann [20] gives it with 5% accuracy for $|\omega| \leqslant 200$ meV, while the magnitude of the self-energy effects is at most a few tenths of a per cent of $\sigma(\omega)$. Probably all deviations from equation (4) are symmetric against zero energy, thus reducing themselves in $\sigma_-(\omega)$. However, one should not assume that the complicated shape of a real barrier leads only to a linear contribution to $\sigma_-(\omega)$. In other words, the inversion of the normal metal tunnelling data is far from being a closed subject. Elimination of the remaining doubts will require further experiments and, possibly, an increase of measurement accuracy.

The elimination of thermal smearing from the normal metal tunnelling conductivity is strongly limited by experimental error. More success should be expected in the case of inelastic tunnelling and point contact spectroscopy, where the thermal smearing function is the same but the experimental error is smaller.

Acknowledgments

The author would like to express his thanks to V M Svistunov and M A Belogolovskii for helpful discussions.

Appendix 1

Both equations (8) and (9) may be directly obtained from the dispersion relation

$$\frac{\mathrm{d}\Sigma_2(\omega)}{\mathrm{d}\omega} = \frac{2\omega}{\pi}\int_0^\infty \frac{\mathrm{d}\sigma_1(\nu)}{\mathrm{d}\nu}\frac{\mathrm{d}\nu}{\omega^2-\nu^2} \tag{A1.1}$$

in place of the originally used relation [1]

$$\Sigma_2(\omega) - \Sigma_2(\infty) = \frac{2}{\pi}\int_0^\infty \frac{\nu\Sigma_1(\nu)}{\omega^2-\nu^2}\,\mathrm{d}\nu. \tag{A1.2}$$

The dispersion relations are due to the analytic properties of the electron self-energy function and its symmetry on the real frequency axis,

$$\Sigma(-\omega) = -\Sigma^*(\omega) \tag{A1.3}$$

$$\mathrm{d}\Sigma(-\omega)/\mathrm{d}\omega = [\mathrm{d}\Sigma(\omega)/\mathrm{d}\omega]^*. \tag{A1.4}$$

Important is the convergence of $\Sigma(\omega)$ is the infinite-frequency limit:

$$\Sigma(\infty) = -inA^2 \tag{A1.5}$$

$$[d\Sigma(\omega)/d\omega]|_{\omega=\infty} = 0. \tag{A1.6}$$

Here

$$A^2 = \int_0^\infty \alpha^2 F(\omega)\, d\omega. \tag{A1.7}$$

Using equation (6) and knowing from (7) that $d\Sigma_2(\omega)/d\omega = -\pi\alpha^2 F(\omega)$, one can directly obtain relation (8).

List of the dispersion relations involved in the inversion methods of normal metal tunnelling data completes the relation obtained from (A1.1) by integration by parts:

$$\frac{d\Sigma_2(\omega)}{d\omega} = -\frac{4\omega}{\pi}\int_0^\infty \frac{\nu\Sigma_1(\omega)}{(\omega^2-\nu^2)^2}\, d\nu. \tag{A1.8}$$

Relation (9) follows from it directly.

The other constants used in this paper are defined as follows:

$$\bar{E} = \int_0^\infty \omega\alpha^2 F(\omega)\, d\omega \tag{A1.9}$$

$$\lambda = 2\int_0^\infty [\alpha^2 F(\omega)/\omega]\, d\omega \tag{A1.10}$$

$$\langle\omega^4\rangle = (2/\lambda)\int_0^\infty \omega^3\alpha^2 F(\omega)\, d\omega \tag{A1.11}$$

Appendix 2

A number of sum rules necessary for the inversion methods to work may be derived from the above three disperion relations ((A1.1), (A1.2), (A1.8)). First of the sum rules listed in table 1 was deduced in [1] from the property $\Sigma_1(0) = \Sigma_1(\infty) = 0$ applied to relation (A1.1). It is also possible to obtain this rule from the so-called superconvergence theorem for the Hilbert transform [25] exploiting the properties of $d\Sigma(\omega)/d\omega$. The next sum rule may be derived either from the explicit form of $\Sigma_1(\omega)$, equation (7) or from one of the relations (A1.2) or (A1.8). The third rule of table 1 is an approximate form of the exact sum rule,

$$\int_0^\infty \frac{\nu\Sigma_1(\nu)}{\nu^2-\omega^2}\, d\nu = 0 \qquad \omega > \omega_0 \tag{A2.1}$$

arising from relation (A1.2). The second sum rule of table 1 within the same approximation (equation (10)) gives rule number 4. (The integrand of rule 4 may seem to have a singularity at $\omega = 0$, but as $\Sigma_1(\omega \to 0) \sim \omega$, the singularity disappears.) The last, fifth, rule of table 1 follows from the first one within approximation (11).

Appendix 3

Defining $z(\omega) \equiv \sigma_-(\omega)$, $g(\omega) \equiv \sigma_-(\omega, T)$ and $H(t) \equiv H(t, T)$, one may rewrite equation (18) in the form:

$$z(\omega) = g(\omega) * h(\omega) = \int \mathrm{d}\nu\, g(\nu) h(\nu - \omega) \tag{A3.1}$$

represented by a multiplication of the respective Fourier transforms, $Z(t) \equiv \mathcal{F}(z(\omega))$, and so on,

$$Z(t) = G(t) \cdot H(t) \tag{A3.2}$$

(to conserve the notation used within this paper, we use a 'time' variable, t, for the forward Fourier transform).

The deconvolution problem comes to division in the 'time' domain:

$$g(\omega) = \mathcal{F}^{-1}\left(\frac{Z(t)}{H(t)}\right) \tag{A3.3}$$

where $\mathcal{F}^{-1}$ denotes a reverse Fourier transform.

Even assuming that the function $H(t)$ is known exactly, there is no guarantee that the above reverse Fourier transform is convergent or that it gives an exact function $g(\omega)$, if the function $z(\omega)$ is noisy (or just inaccurate).

The regularization method introduces a stabilization factor, $s(t, \alpha)$, into the above equation,

$$g(\omega) = \mathcal{F}^{-1}\left(\frac{Z(t)}{H(t)} s(t, \alpha)\right). \tag{A3.4}$$

(In practice, $s(t, \alpha)$ is used to damp the function $Z(t)/H(t)$ for high values of t.)

The stabilization factor has to fulfil a set of conditions, which will not be discussed here. For the specific case presented in this paper we have chosen the function of the form:

$$s(t, \alpha) \equiv \frac{H(t)}{H(t) + \alpha[1 - H(t)]} \tag{A3.5}$$

where α is a regularization parameter, $0 \leqslant \alpha \leqslant 1$. It is obvious that for $\alpha = 0$, $s(t, \alpha) = 1$ and no regularization is performed. On the other hand, for $\alpha = 1$, we have $g(\omega) = z(\omega)$ and no thermal smearing is being removed from $\sigma_-(\omega, T)$ as the deconvolution does not take place.

There exists a unique value of $\alpha < 1$ for which the absolute error of $z(\omega)$, δ, fulfils the equation [26]:

$$\delta^2 = \frac{1}{2\pi} \int_{-\infty}^{\infty} |Z(t)[1 - s(t, \alpha)]|^2 \,\mathrm{d}t \tag{A3.6}$$

or its equivalent

$$\delta^2 = \frac{1}{2\pi} \int_{-\infty}^{\infty} \frac{\alpha^2 [1 - H(t)]^2 |Z(t)|^2}{\{H(t) + \alpha[1 - H(t)]\}^2} \,\mathrm{d}t. \tag{A3.7}$$

Fortunately, the value of δ may be calculated as the weighted sum of Fourier coefficients, z_i, of $z(\omega)$. In the simplest case, (A3.7) reduces to the equality:

$$\sum_{i=N_m+1}^{N} |z_i|^2 = \alpha^2 \sum_{i=0}^{N} \frac{(1-h_i)^2|z_i|^2}{[h_i+\alpha(1-h_i)]^2} \tag{A3.8}$$

where h_i are the Fourier coefficients of $h(\omega)$, N is the number of transform points, and N_m is the closest integer to $N/2$. (The proper calculation of the Fourier transform and the ill-conditioned rpoblem of summation of its coefficients form a separate subject, which will be not addressed here.)

The elimination of the thermal smearing starts with $\alpha = 1$. Comparison of both sides of (A3.8) shows whether the elimination may be performed. If the right-hand side is the smaller one, then alpha may be consecutively reduced until the equality is reached with assumed accuracy. We have used the bisection algorithm in finding the optimal value of the regularization parameter. In effect, one obtains a reduction of the thermal smearing to the extent determined by the accuracy of the initial data—and the convenient choice of the stabilization factor allows one to estimate the amount of this reduction from the value of α.

Another consequence of the convenient choice of the stabilization factor, $s(t, \alpha)$, is that it may not be 'strong' enough to give a smooth function $z(\omega) = \sigma_-(\omega)$ for all possible values of temperature and experimental error. In fact, we have used the properties of the regularization method to form a more general algorithm, allowing processing of data disturbed by noise, which exploits stabilization factors of different kinds—depending on the amplitude of the experimental error. This algorithm was used separately in cases when the reduction of thermal smearing was not necessary, or simultaneously with the one described above.

References

[1] Svistunov V M, Belogolovskii M A, Chernysh O I, Khachaturov A I and Kvachev A P 1983 *Zh. Eksp. Teor. Fiz.* **84** 1781
[2] Herman H and Shmid A 1986 *Z. Phys.* **211** 313
[3] Rowell J M, McMillan W L and Feldman W L 1969 *Phys. Rev.* **180** 658
[4] Burrafato F, Faraci C, Giaquinta G and Mancini N 1972 *J. Phys. C: Solid State Phys.* **5** 2179
[5] Chernyak O I, Khachaturov A I and Kvachev A P 1984 *J. Phys. F: Met. Phys.* **14** 2359
[6] Appelbaum J A and Brinkman W F 1969 *Phys. Rev.* **183** 553
[7] Davis L C 1969 *Phys. Rev.* **187** 1177
[8] Leavens C R 1985 *Solid State Commun.* **55** 13
[9] Inavchenko Yu M and Medvedev Yu V 1973 *Zh. Eksp. Teor. Fiz.* **64** 1024
[10] Belogolovskii M A, Ivanchenko Yu M and Medvedev Yu V 1975 *Pis. Zh. Eksp. Teor. Fiz.* **21** 701
[11] Belogolovskii M A, Ivanchenko Yu M and Medvedev Yu V 1975 *Fiz. Verd. Tela.* **17** 2907
[12] Ivanchenko Yu M and Medvedev Yu V 1976 *Fiz. Nizk. Temp.* **2** 141
[13] Mitrović B and Carbotte J P 1983 *Can. J. Phys.* **61** 758
[14] Leavens C R and Mitrović B 1985 *Physica* B **135** 208
[15] Rowell J M and McMillan W L 1971 *Phys. Rev.* B **2** 4065
[16] Hertel G B and Orlando T P 1984 *Proc. 14th Int. Conf. on Low Temperatures Physics* (Amsterdam: North-Holland) p 841
[17] Leavens C R 1985 *Solid State Commun.* **54** 625
[18] Wnuk J J 1988 *Phys. Status Solidi* b **146** K91
[19] Scalapino D J 1969 *Superconductivity* ed R D Parks (New York: Marcel Dekker) p 449
[20] Brinkman W F, Dynes R C and Rowell J M 1970 *J. Appl. Phys.* **41** 1915
[21] Walmsley D G, Floyd R B and Timms W E 1977 *Solid State Commun.* **22** 497
[22] Lambe J and Jakevic L C 1966 *Phys. Rev.* **165** 821

[23] Klein J, Leger A, Belin M, Defourneau D and Sangster M J L 1973 *Phys. Rev.* B **7** 2336
[24] Hansma P K 1982 *Tunneling Spectroscopy* ed P K Hansma (New York: Plenum) p 4
[25] Altarelli M, Dexter D L and Nussenzveig H N 1972 *Phys. Rev.* B **6** 4502
[26] Tikhonov A and Arsenin V 1979 *Methods of Solving Ill-Conditioned Problems* 2nd edn (Moscow: Nauka) in Russian
[27] Adler J G, Kreuzer H J and Wattamaniuk W J 1971 *Phys. Rev. Lett.* **27** 185
[28] Wattamaniuk W J, Kreuzer H J and Adler J G 1971 *Phys. Lett.* **37A** 7
[29] Knorr K and Barth N 1970 *Solid State Commun.* **8** 1085
[30] Rowell J M, McMillan W L and Dynes R C 1971 *A Tabulation of the Electron–Phonon Interaction in Superconducting Metals and Alloys. Part I* unpublished (drawings may be found in: McMillan W L and Rowell J M 1969 *Superconductivity* ed R D Parks (New York: Dekker) p 561)
[31] Geerk J private communication